



Study of Coanda effect in turbulent jets

Binayak Lohani

Bachelor's in Aerospace Engineering

Department of Mechanical and Aerospace Engineering Pulchowk Campus,
Lalitpur, Nepal

Abstract

The objective of the present project is to study Coanda effect in turbulent jets for different viscous fluids in open source CFD package OpenFOAM. Coanda Effect is the phenomena in which jet flow attaches itself to a nearby surface and flow along it. Coanda effect for H_2O , D_2O , Cooking oil, Motor oil (SAE 30 and SAE 50) is studied in gravity driven flow with flowrate inlet boundary condition. This project also explains setting up OpenFOAM case from existing tutorials available in the OpenFOAM repository along with meshing and post-processing methodologies.

Keywords: OpenFOAM, CFD, Coanda effect

1. Introduction

The Coanda Effect is the tendency of any fluid to adhere or attach and follow the curvature of the surface in which the fluid flows. This effect was first noticed by a Romanian inventor, Henry Coanda in 1910 in a rectangular nozzle and the fluid ejected was air. He observed that air would attach to the inclined surface of the rectangular nozzle.

Coanda Effect is mainly caused due to two major factors which are the curvature of the surface where fluid is flowing and the other major factor is the attachment of working fluid with the curved surface for which viscous effects needs to be considered for further understanding of the effect. Therefore, in this project we will study the effect of viscosity of the working fluid on Coanda Effect.

2. Problem Statement

The primary aim of the project is to capture and study the angle of deflection of the fluid in the curved surface of cylinder for different viscous fluids and evaluate the effect of viscosity on Coanda effect. The entire domain is initially filled with air and working fluid is made to enter the domain from the inlet. Figure 1 shows the geometry of physical domain considered:

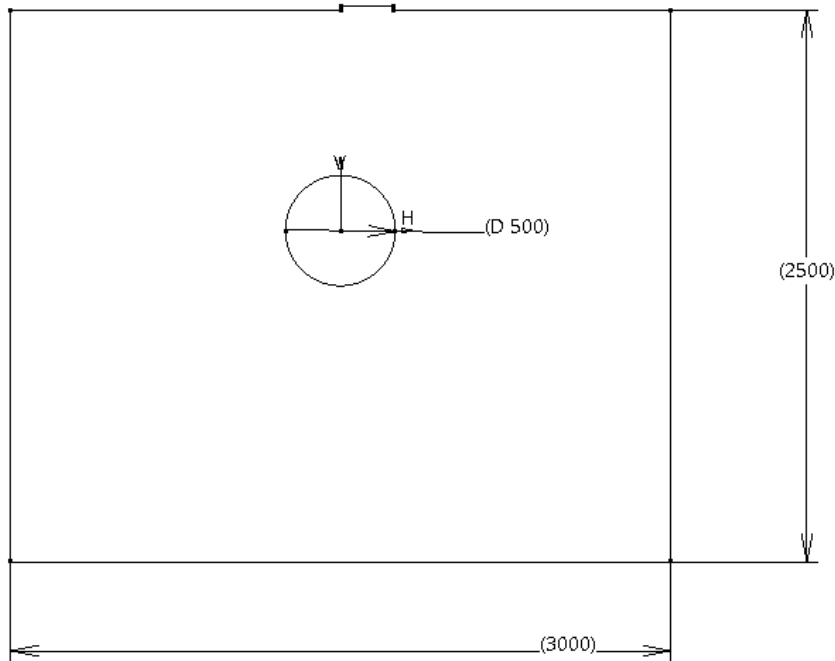


Figure 1: Geometry used for the simulation (Dimensions are in mm)

3. Governing Equations

The governing equations for the fluid flow can be written in differential form as follows:

- Conservation of Mass

$$\frac{\partial \rho}{\partial t} + \Delta \cdot (\rho U) = 0$$

3.1.a

- Conservation of Momentum

In x-direction

$$\frac{\partial \rho u}{\partial t} + \frac{\partial \rho u u}{\partial x} + \frac{\partial \rho u v}{\partial y} + \frac{\partial \rho u w}{\partial z} = -\frac{\partial p}{\partial x} + \frac{\mu \partial}{\partial x} \left(\frac{\partial u}{\partial x} + \frac{\partial u}{\partial y} + \frac{\partial u}{\partial z} \right) + \rho f_x$$

In y-direction

$$\frac{\partial \rho v}{\partial t} + \frac{\partial \rho v u}{\partial x} + \frac{\partial \rho v v}{\partial y} + \frac{\partial \rho v w}{\partial z} = -\frac{\partial p}{\partial y} + \frac{\mu \partial}{\partial y} \left(\frac{\partial v}{\partial x} + \frac{\partial v}{\partial y} + \frac{\partial v}{\partial z} \right) + \rho f_y$$

In z-direction

$$\frac{\partial \rho w}{\partial t} + \frac{\partial \rho w u}{\partial x} + \frac{\partial \rho w v}{\partial y} + \frac{\partial \rho w w}{\partial z} = -\frac{\partial p}{\partial z} + \frac{\mu \partial}{\partial z} \left(\frac{\partial w}{\partial x} + \frac{\partial w}{\partial y} + \frac{\partial w}{\partial z} \right) + \rho f_z$$

3.1.b

Equations 3.1.a and 3.1.b along with energy equation (not solved here) constitutes as Navier-Stokes equations. The given equations are to be discretized in space and solve them with the help of governing equations.

3.1 Volume of Fluid (VOF) model

Volume of Fluid model was presented by Hirt and Nichols (1981) which is used for multiphase simulation where α is the volume fraction parameter used to define which portion of the discretized cell is occupied by which fluid.

$$\begin{aligned} \alpha &= 1 && \text{(volume occupied by the fluid 1)} \\ &= 0 < \alpha < 1 && \text{(volume fraction at the interface)} \\ &= 1 && \text{(volume occupied by the fluid 2)} \end{aligned} \tag{3.1.1}$$

Transportation of α in time can be expressed as:

$$\frac{\partial \alpha}{\partial t} + \nabla \cdot (\alpha u) = 0 \tag{3.1.2}$$

The subscripts 1 and 2 denote different fluids.

$$\rho = \alpha \rho_1 + (1 - \alpha) \rho_2 \tag{3.1.3}$$

$$\mu = \alpha \mu_1 + (1 - \alpha) \mu_2 \tag{3.1.4}$$

ρ and μ are the weighted density and viscosity of the mixture of two fluids.

3.2 Surface Tension Force

Surface tension force is the force which acts between the interface between two phases. In order to capture the interface, we need to take care of viscous stress term and surface tension, hence the momentum equation can be written as:

$$\frac{\partial \rho u}{\partial t} + \nabla \cdot (\rho u u) - \nabla \cdot (\mu \nabla u) = -\nabla p^* + (\nabla u) \cdot \nabla \mu - g \cdot x \nabla \rho + \sigma \kappa \nabla \alpha \quad 3.1.7$$

where, σ is the surface tension coefficient and κ is curvature of the surface.

3.3 Turbulence Modelling

The flow which is smooth and where adjacent layers of fluid flows in orderly fashion is known as laminar flow whereas the chaotic flow in the fluid is the turbulent flow. The main reason behind choosing the flow to be turbulent was to model the frictional surface of the cylinder with the help of `nutkRoughWallFunction` boundary condition for turbulent viscosity at the curved surface. We chose the flow to be turbulent since the Reynold's number. Turbulence modelling is required for simulating the turbulent flow because Direct Numerical Simulation (DNS) needs huge computational power. Hence, the turbulent model which are available are Large Eddy Simulation (LES), Detached Eddy Simulation (DES), Reynold's Averaged Navier Stoke (RANS), etc. Since, RANS offers less computational power than any other modelling problem, it is largely used on most of the CFD problems. According to [5], for the $k-\omega$ SST model, the separation location was slightly closer to the experimental data. Therefore, $k-\omega$ SST model is chosen for the case study.

4. Simulation Procedure

Three folders namely 0, constant and system are needed to conduct simulation in OpenFOAM.

0 : Defines the initial and boundary condition of the domain, eg. pressure, velocity, phase fraction, etc

Constant : Contains grid information, defines turbulent models used and transport properties to describe the properties of the fluid.

System : Defines the solver to be used and controls the simulation parameters for convergence.

Fluid	Denisty (ρ , kg/m ³)	Kinematic Viscosity (ν , m ² /s)	Surface Tension for air interface (γ , N/m)
H_2O at 20°C	1000	$1 * 10^{-6}$	0.072
D_2O at 20°C	1107	$1.2 * 10^{-6}$	0.071
Cooking Oil	920	$4.32 * 10^{-5}$	0.033
Motor Oil (SAE 30 oil)	875	$4.4 * 10^{-4}$	0.036
High viscous fluid (SAE 50 oil)	892	$1.7335 * 10^{-3}$	0.034

Table 1: Material Properties of different fluids used

4.1 Geometry and Mesh

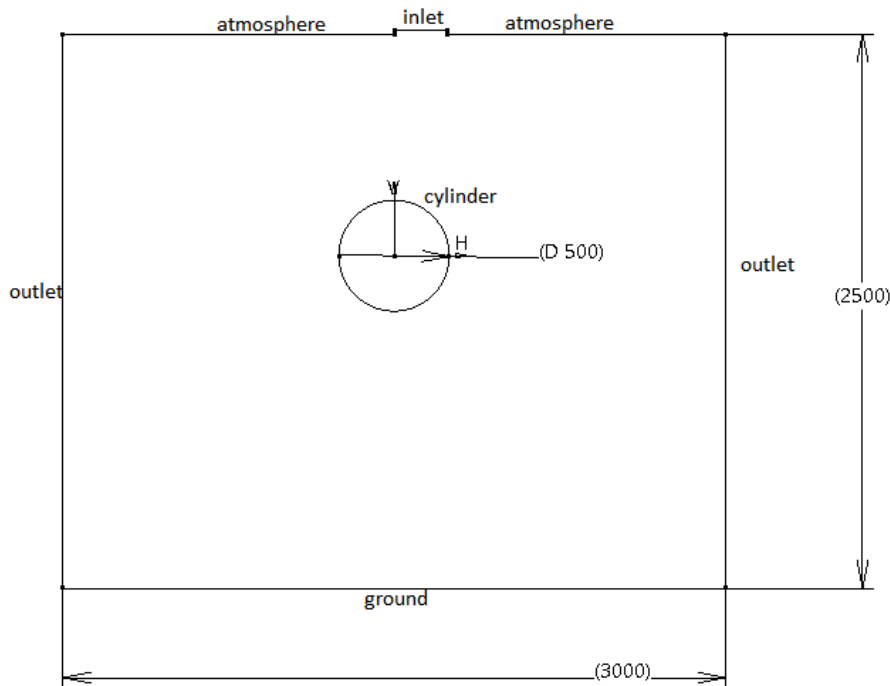


Figure 2: Geometry and boundaries used for the simulation

The diameter of the circular cylinder is 500mm and the inlet for the fluid is shifted right from the center. Since, OpenFOAM works only on three dimensional geometry, created two-dimensional geometry is extruded in the third direction. The domain size for the geometry is 2500×3000 mm. The domain of interest needs to be discretized so that the governing equations is formulated at each created cells. The most important task for achieving a good results in CFD is involved in creation of good grid which can be examined with many parameters some of which is listed below:

A good grid quality results in the accurate convergence of the solution. The grid has a significant impact on:

- Rate of convergence of the solution.
- Accuracy of the solution.
- CPU time required.

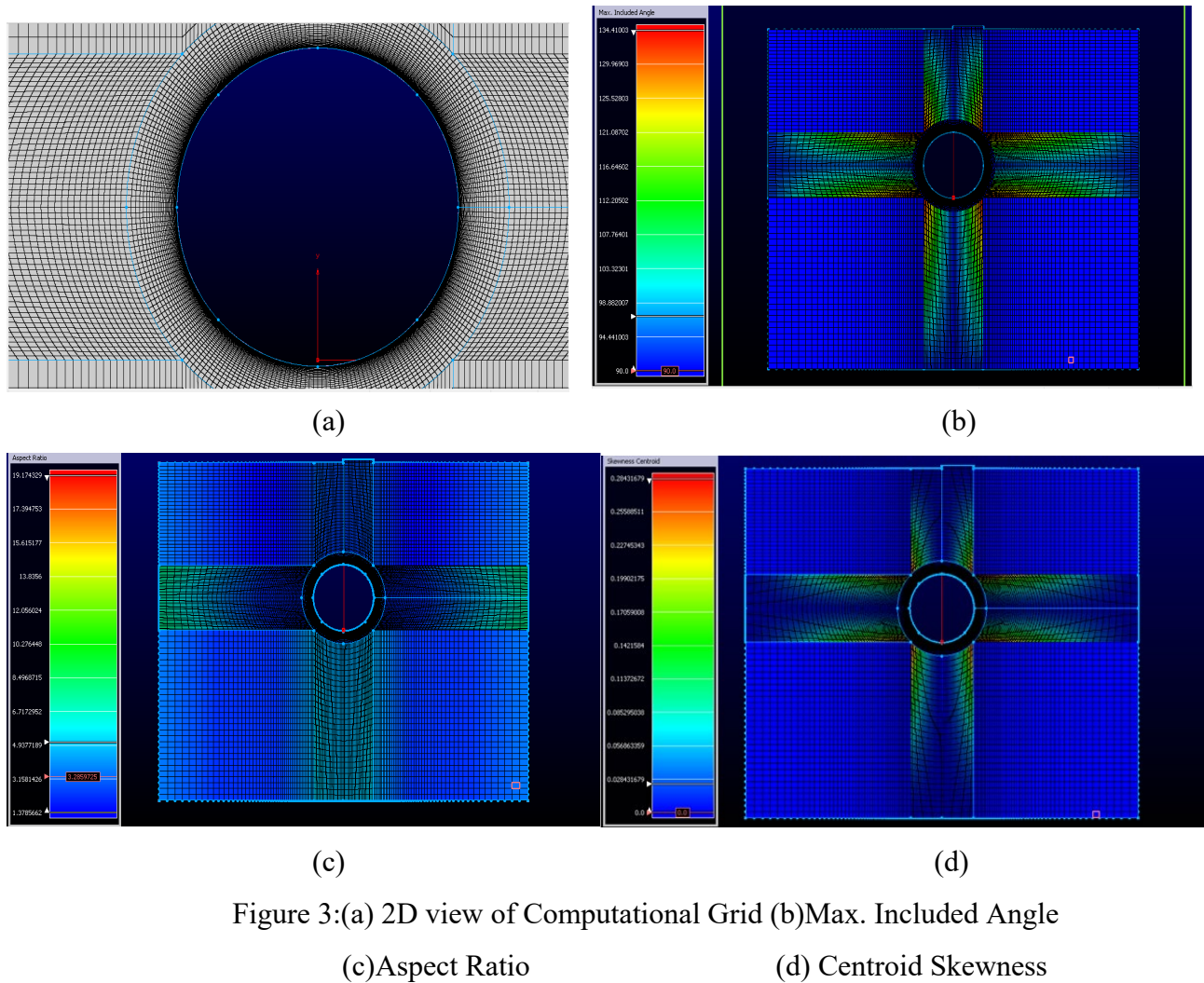
There are two types of grid that can be made which are as follows:

- Structured and
- Unstructured grid

Structured grids being difficult to construct provides more accurate results than the unstructured grids. Since, the domain of interest for meshing is a simple geometry, structured grids can be created with ease. The grid generation could be done in OpenFOAM itself which has its own meshing tool known as blockMesh and snappyHexMesh. This tool is implemented with the help of code directly so, it becomes tedious and difficult task to create a good quality mesh in such a geometry. Hence, a well-known commercial meshing software known as Pointwise is used to generate better quality grid.

4.1.1 Pointwise

Pointwise is one of the top commercial software for grid generation for computational fluid dynamics (CFD), and other numerical simulations. Pointwise has the ability of generating high quality mesh both manually and automatically. For a geometry as such used in this project it requires to take more manual steps to increase its quality. The mesh generated can be seen below:



To solve the laminar sublayer for the turbulence models, the y^+ values of the wall next grid points was 1, and the $x^+ \Delta$ values was 50. The created mesh must be examined properly so that convergence criteria is acquired. Some of the mesh properties that must be checked are maximum and minimum included angle, aspect ratio, centroid skewness, etc. The maximum included angle for the mesh generated is 134.41° . For the mesh included angle less than 175° , the mesh is considered to be of good quality. The maximum aspect ratio for the mesh is 19 for which the mesh can be considered of good quality. Centroid skewness is one of the important parameter to be examined in Pointwise for the solver which is OpenFOAM. Centroid skewness of less than 1 is considered of a good quality and hence, mesh with 0.28 of maximum centroid skewness can be considered good for convergence.

The created mesh can be directly exported to OpenFoam which already contains all the necessary files required for the solver and hence, those file are to be copied in the polyMesh directory inside constant folder. Files generated using Pointwise is provided in the case files separately also.

	Selection	Entire Grid
Connectors		
Total Cells	0	3,050
Total Points	0	2,988
Domains		
Triangles	0	0
Quads	0	44,311
Total Cells	0	44,311
Total Points	0	43,816
Blocks		
Tets	0	0
Pyramids	0	0
Prisms	0	0
Hexes	21,518	21,518
Total Cells	21,518	21,518
Total Points	43,816	43,816

Figure 4: Computational Grid Size

Hence, the mesh was created using Pointwise having about 21 thousand cells.

4.2 Initial and Boundary Condition

Initial and Boundary condition become very important to differentiate different case study problems, hence it is essential to define them accurately to achieve the desired results. To complete the problem, it is essential to define the boundary and the initial conditions.

Initial and Boundary Conditions are defined for the following properties:

	Velocity (U)[m/s]	Pressure (p_rgh)	nut	k	omega
inlet	flowRateInletVelocity(1e05)	fixedFluxPressure	fixedValue	fixedValue	fixedValue
atmosphere	pressureInletOutletVelocity	totalPressure	zeroGradient	inletOutlet	inletOutlet
outlet	zeroGradient	zeroGradient	zeroGradient	inletOutlet	inletOutlet
cylinder	noSlip	zeroGradient	nutkRoughWallFunction	kqRWallFunction	omegaWallFunction
inletwall	noSlip	zeroGradient	nutkWallFunction	kqRWallFunction	omegaWallFunction
ground	noSlip	zeroGradient	nutkWallFunction	kqRWallFunction	omegaWallFunction
frontback	empty	empty	empty	empty	empty

Table 2: Boundary Conditions

The flow region will be split with the fluid 1 at the inlet and rest of the geometry with fluid 2 using setFields utility to initialize the non-uniform initial condition.

4.3 Constant Properties of the system

The constant properties of the system defines various characteristics defining mesh information, transport properties, turbulence properties and gravity effects in each of their own folder as follows:

- **polyMesh**

the polyMesh folder contains the mesh information which is imported from Pointwise as specified earlier. We do not need to alter it.

- **transportProperties**

This file contains the information about the physical properties of the working fluid such as density, viscosity and surface tension between the two phases. These properties are provided at table no. 1.

- **turbulenceProperties**

This file contains the information about the turbulence properties of the system. Since Reynold's Averaged Simulation (RAS) $k-\omega$ SST is chosen for turbulence modelling, the properties are described accordingly.

- **g**

In OpenFOAM the gravity is a uniform vector field across the computational domain and can be set in the dictionary g. The absolute value of the gravity is always 9.8 m/s^2 in every case which is set as (0 - 9.8 0) along the y-direction.

4.4 Setting the runtime conditions and output control

The simulation controls like starting and end time, discretization, interpolation and solution schemes, and other parameters can be controlled by altering the controlDict, fvSchemes and fvSolution files in the system directory of the case folder.

- **controlDict**

This file contains starting and ending time, time step size, maximum courant number allowed. The running time is taken as 200 seconds with an initial time step of 0.1.

- **fvSchemes**

This file contains the information about the discretization and interpolation schemes for various mathematical expressions such as gradient, Laplacian terms, etc along with temporal discretization.

- **fvSolution**

This file contains the information about the solver to be used, tolerance and solution algorithms.

- **setFieldsDict**

This dictionary file is used to initialize the fluid position.

4.5 Solver

The simulation is meant to be a multiphase problem. Thus, the solver needed has to be able to deal with these kinds of problems. The solver used in this case is called `interFoam`. `interFoam` is a twophase solver for incompressible, isothermal and immiscible fluids. When using `interFoam`, the phase fraction varies from 0 to 1 which is described in 3.1.1. `interFoam` uses PIMPLE algorithm to solve the coupling problem in the fluid flow.

4.6 Pimple algorithm

The PIMPLE algorithm is a combination of the PISO and SIMPLE algorithms. It is used to couple the pressure and momentum quantities for fulfilling the mass conservation. The PIMPLE algorithm allows for transient calculation at larger courant numbers i.e (< 1), which allows for bigger time steps.

5. Results and Discussions

All the simulations were run on a machine using intel Core i5 and 8 Gigabytes of memory on 4 cores. ParaView which is an open-source visualization software is used for post-processing. ParaView is launched by writing `paraFoam` in the terminal. During post-processing, angle (θ) in degrees is represented at the interval of -90° to 90° in a perodic manner for a circular cylinder which has to be interpreted in terms of 0° to 360° for ease.

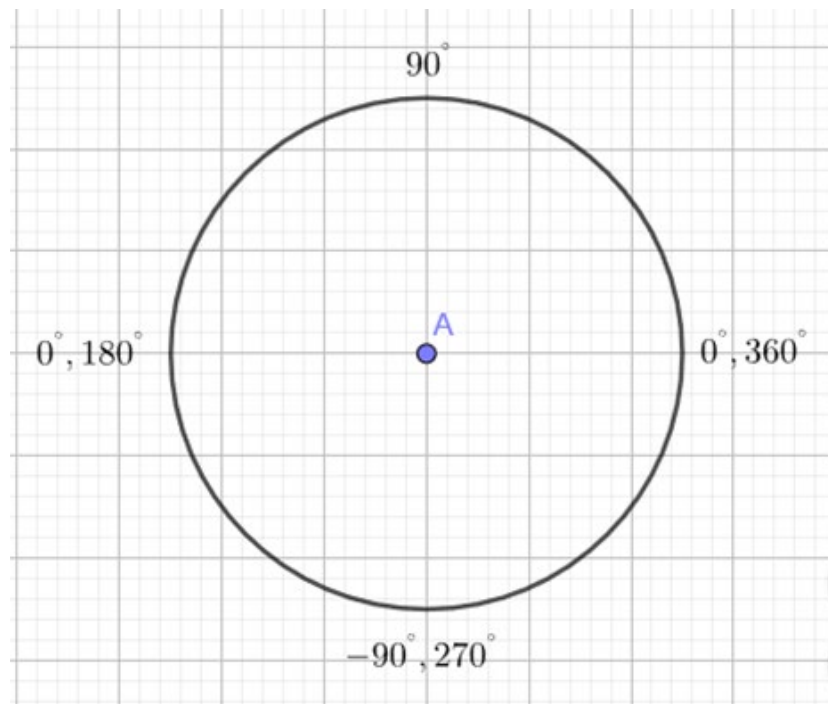
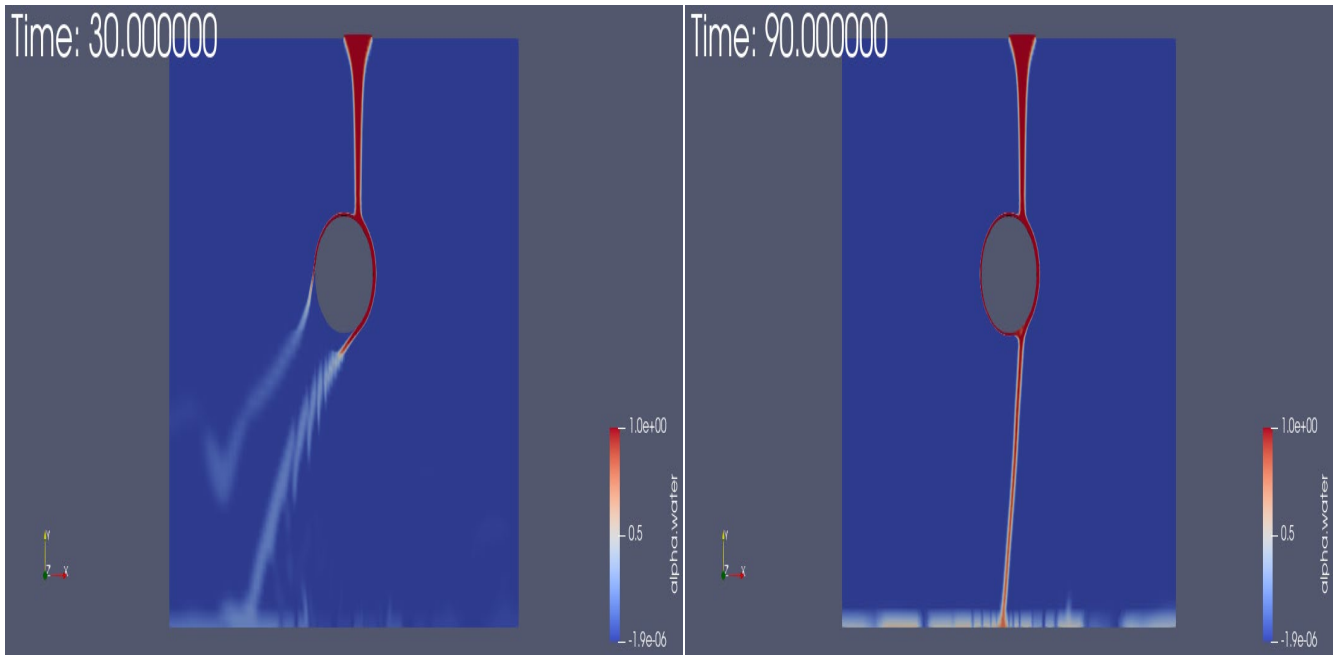


Figure 5: Representation of angle (in degrees) for a circular cylinder

Following results have been obtained :

5.1 H_2O as a working fluid



(a) $t=30s$

(b) $t=90s$

Figure 6: Phase fraction of H_2O at different time

We can see that entrainment of fluid (H_2O) in the circular cylinder in different time stamps at 30 and 90 seconds respectively. At 90 second, H_2O is attached to the cylinder completely and follow the curved surface on both sides.

Hence, time 30 second is chosen for the entrainment of fluid to the surface for comparison.

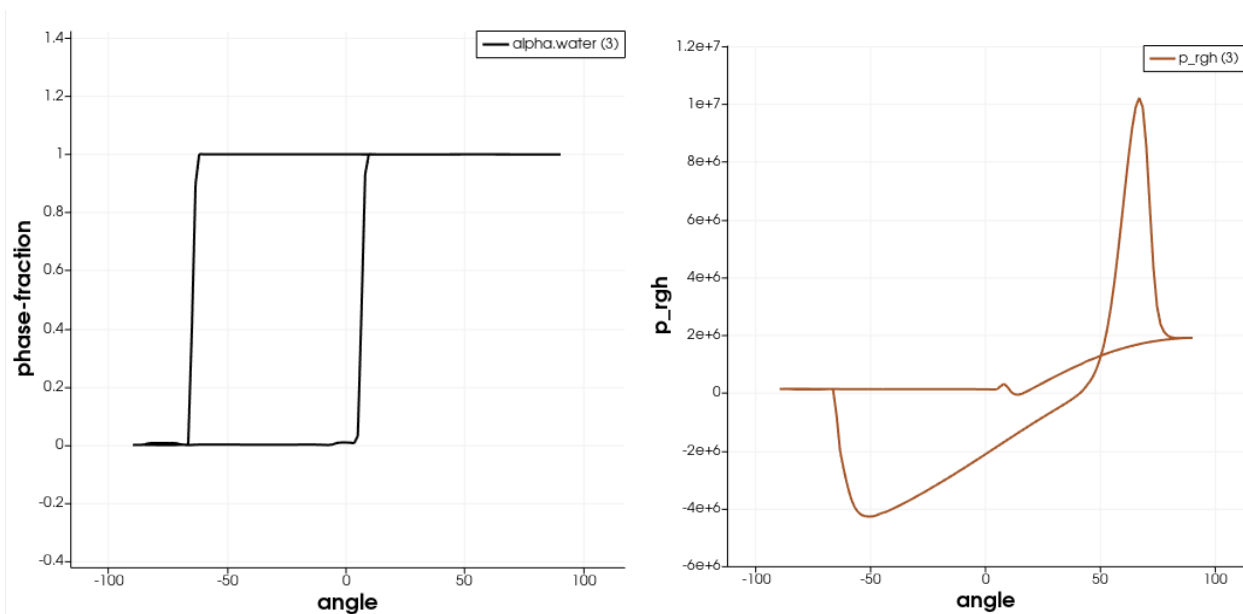


Figure 7: Plot of phase fraction(α) and hydrostatic pressure vs angle (θ)

Hydrostatic pressure and phase fraction is plotted against angle of cylinder as shown in Figure. 5 in order to study the angle of separation of fluid from the curved surface of the cylinder. Adverse pressure gradient and low value of phase fraction may be the indicator to know the angle of separation. Hence, from the plot it can be observed that at $\theta_1 = 10^\circ$ (or equivalently 170°) and $\theta_2 = -55^\circ$ (or equivalently 305°), i.e.at 170° and 305 fluid is separated at this point at 30 second.

5.2 D_2O as a working fluid

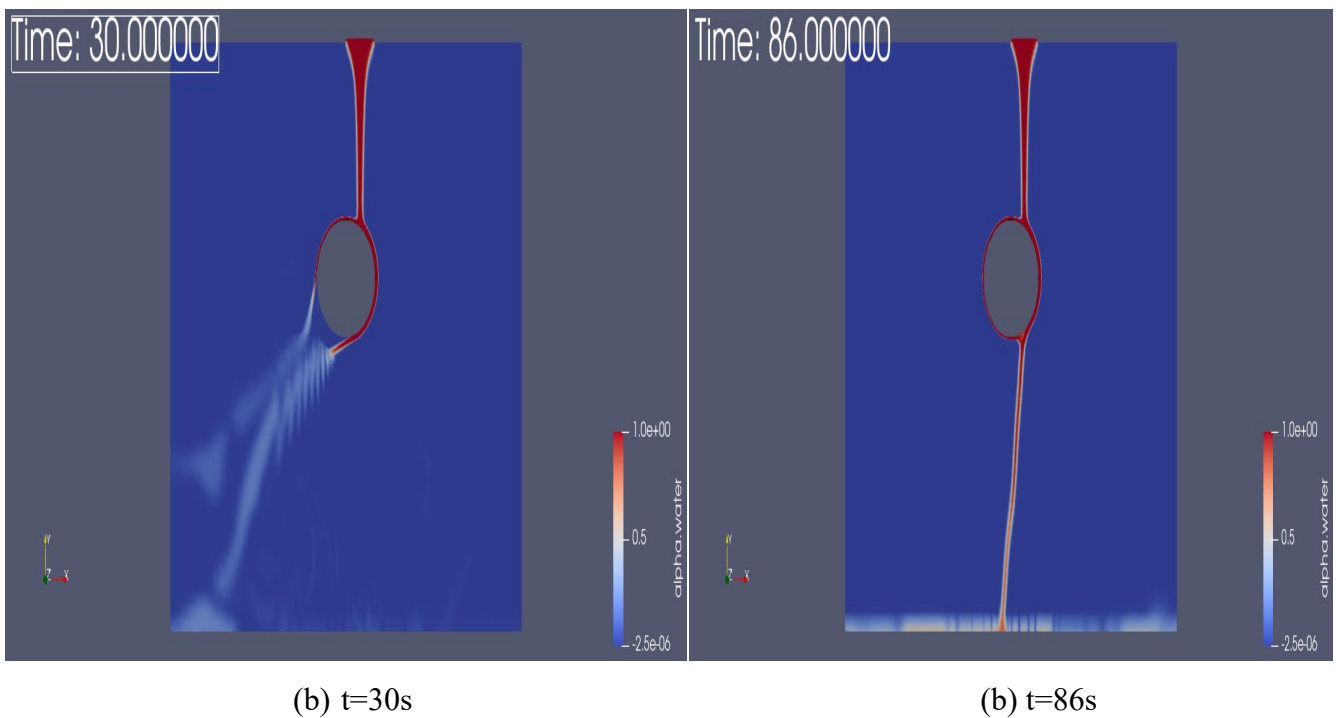


Figure 8: Phase fraction of D_2O at different time

We can see that entrainment of fluid (D_2O) in the circular cylinder in different time stamps at 30 and 90 seconds respectively. At 86 second, D_2O is attached to the cylinder completely and follow the curved surface on both sides.

Hence, time 30 second is chosen for the entrainment of fluid to the surface for comparison.

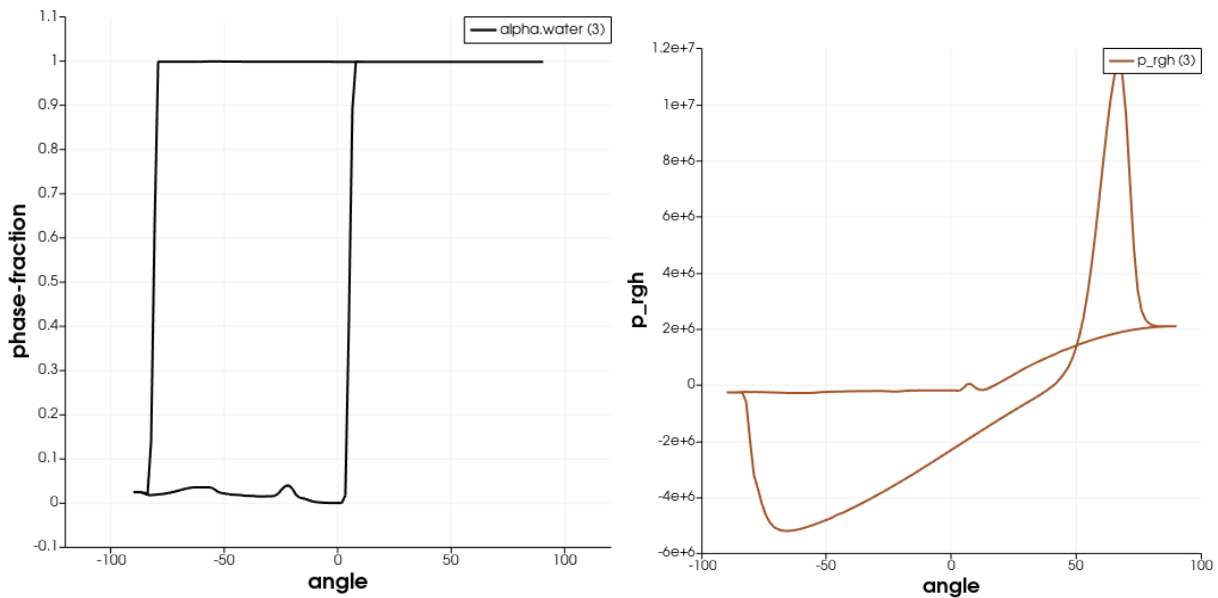
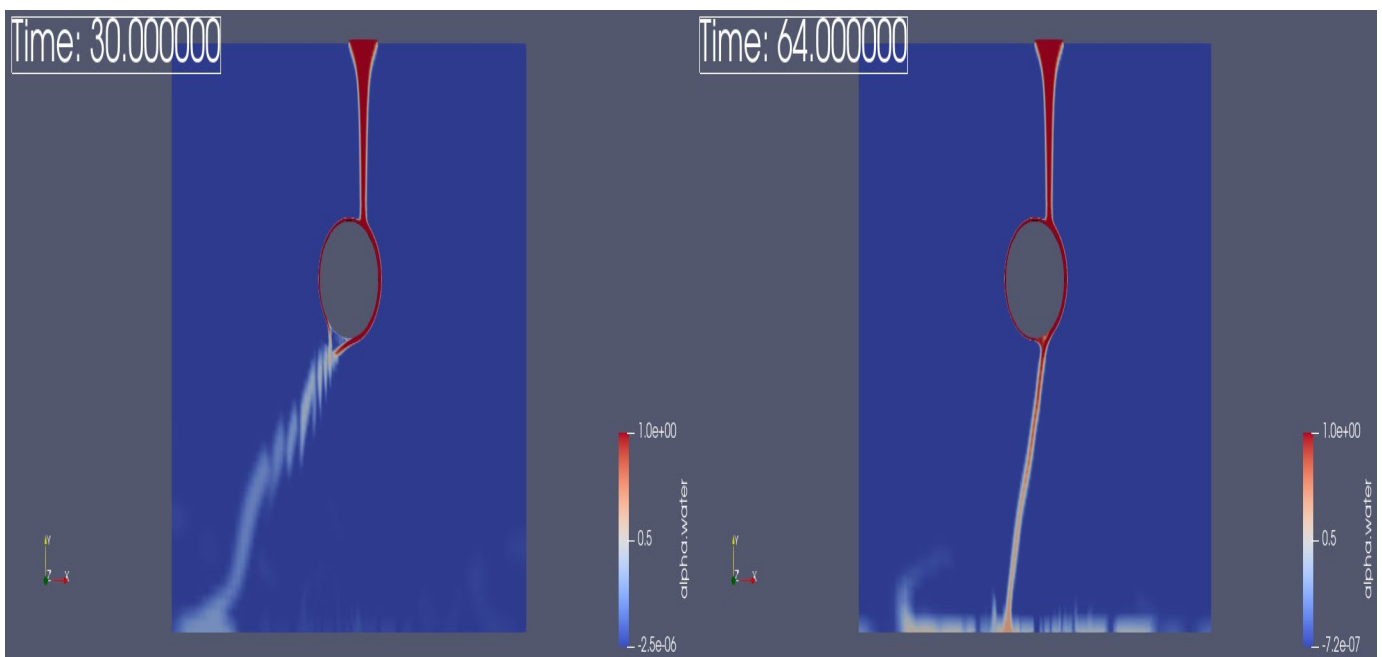


Figure 7: Plot of phase fraction(α) and hydrostatic pressure vs angle (θ)

Hydrostatic pressure and phase fraction is plotted against angle of cylinder as shown in Figure. 5 in order to study the angle of separation of fluid from the curved surface of the cylinder. Adverse pressure gradient and low value of phase fraction may be the indicator to know the angle of separation. Hence, from the plot it can be observed that at $\theta_1 = 9^\circ$ (or equivalently 171°) and $\theta_2 = -70^\circ$ (or equivalently 290°), i.e.at 171° and 290° fluid is separated at this point at 30 second.

5.3 Cooking Oil as a working fluid



(c) $t=30s$

(b) $t=64s$

Figure 9: Phase fraction of cooking oil at different time

We can see that entrainment of fluid (cooking oil) in the circular cylinder in different time stamps at 30 and 90 seconds respectively. At 64 second, cooking oil is attached to the cylinder completely and follow the

curved surface on both sides. Hence, time 30 second is chosen for the entrainment of fluid to the surface for comparison.

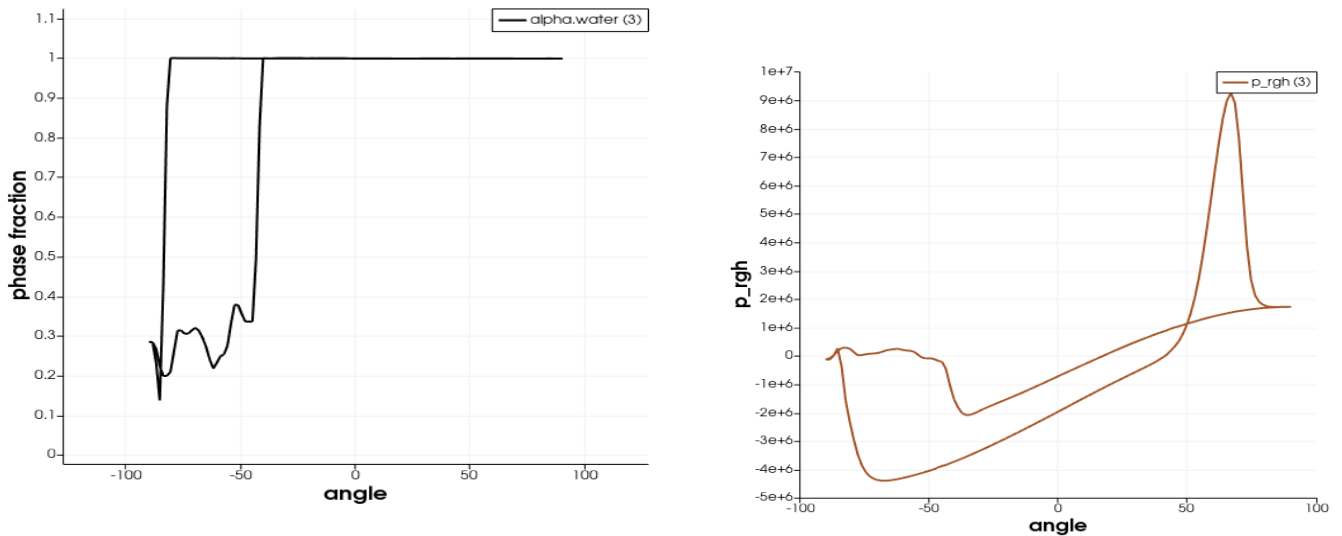


Figure 10: Plot of phase fraction(α) and hydrostatic pressure vs angle (θ)

Hydrostatic pressure and phase fraction is plotted against angle of cylinder as shown in Figure. 5 in order to study the angle of separation of fluid from the curved surface of the cylinder. Adverse pressure gradient and low value of phase fraction may be the indicator to know the angle of separation. Hence, from the plot it can be observed that at $\theta_1 = -37^\circ$ (or equivalently 217°) and $\theta_2 = -71^\circ$ (or equivalently 289°), i.e.at 217° and 289° fluid is separated at this point at 30 second.

5.4 SAE 30 as a working fluid

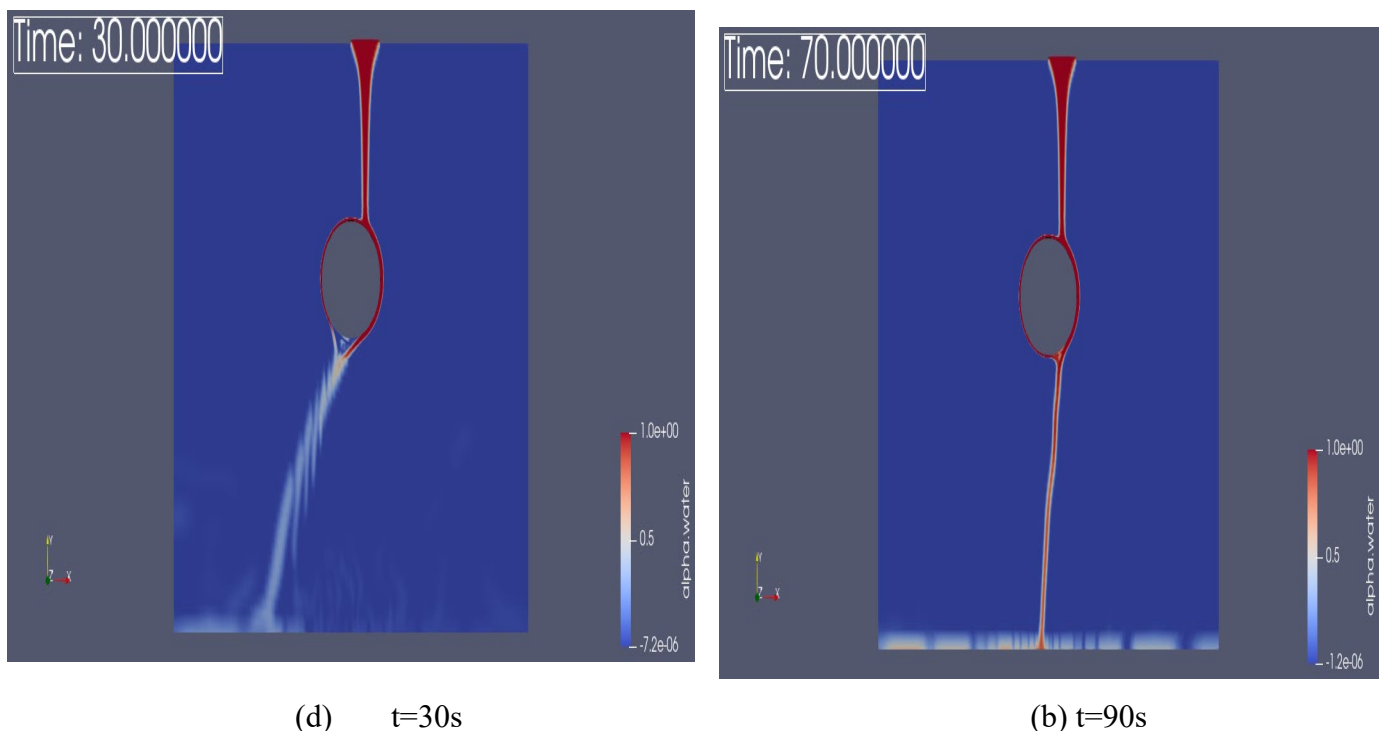


Figure 11: Phase fraction of SAE-30 at different time

We can see that entrainment of fluid (SAE-30) in the circular cylinder in different time stamps at 30 and 90 seconds respectively. At 70 second, SAE-30 is attached to the cylinder completely and follow the curved surface on both sides.

Hence, time 30 second is chosen for the entrainment of fluid to the surface for comparison.

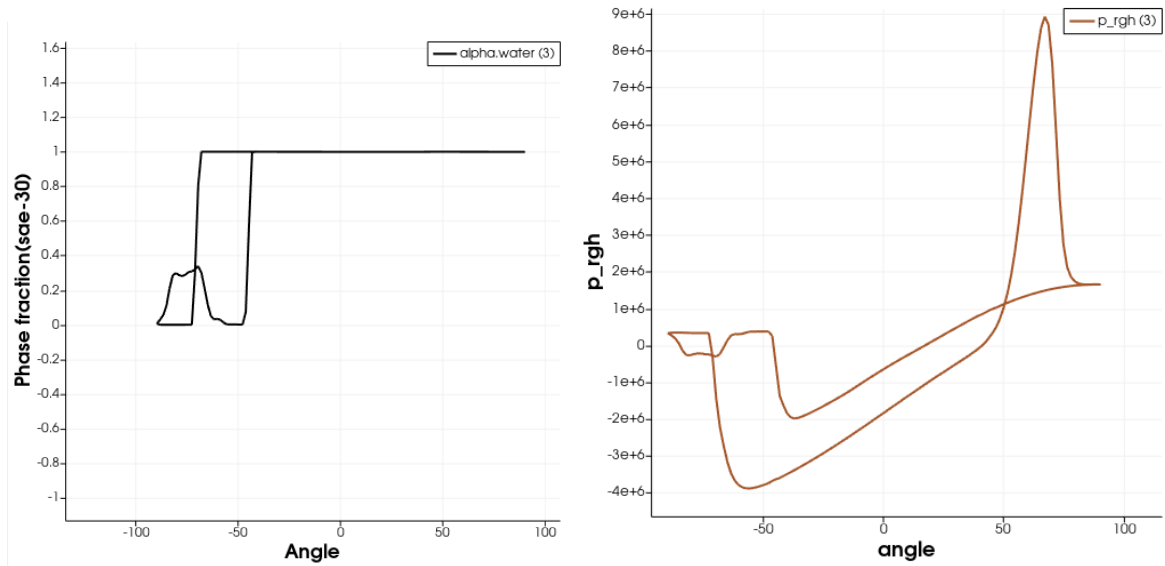
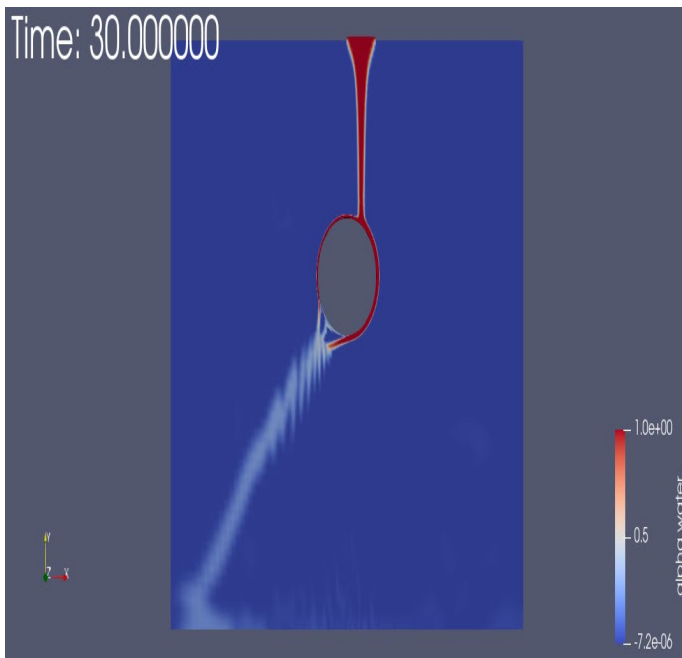


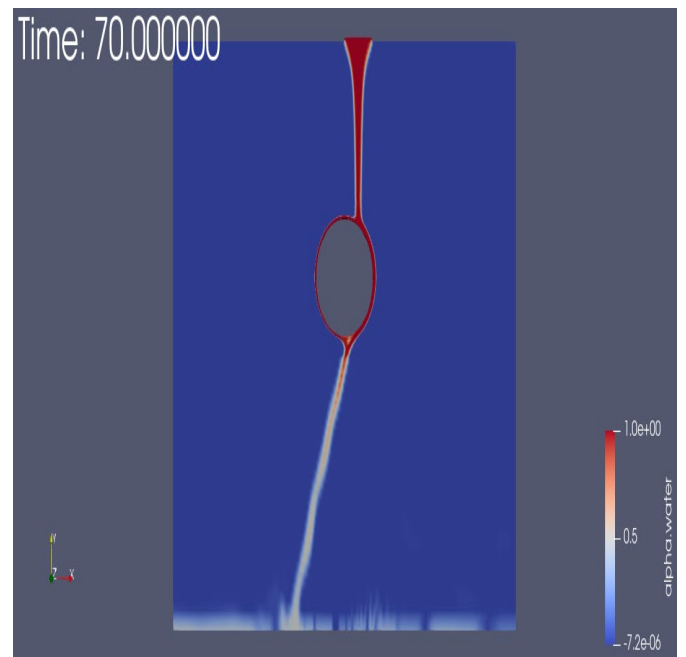
Figure 12: Plot of phase fraction(α) and hydrostatic pressure vs angle (θ)

Hydrostatic pressure and phase fraction is plotted against angle of cylinder as shown in Figure. 5 in order to study the angle of separation of fluid from the curved surface of the cylinder. Adverse pressure gradient and low value of phase fraction may be the indicator to know the angle of separation. Hence, from the plot it can be observed that at $\theta_1 = -40^\circ$ (or equivalently 220°) and $\theta_2 = -60^\circ$ (or equivalently 300°), i.e.at 220° and 300° fluid is separated at this point at 30 second.

5.5 SAE 50 as a working fluid



(e) $t=30s$



(b) $t=70s$

Figure 13: Phase fraction of SAE-50 at different time

We can see that entrainment of fluid (SAE-50) in the circular cylinder in different time stamps at 30 and 90 seconds respectively. At 70 second, SAE-50 is attached to the cylinder completely and follow the curved surface on both sides.

Hence, time 30 second is chosen for the entrainment of fluid to the surface for comparison.

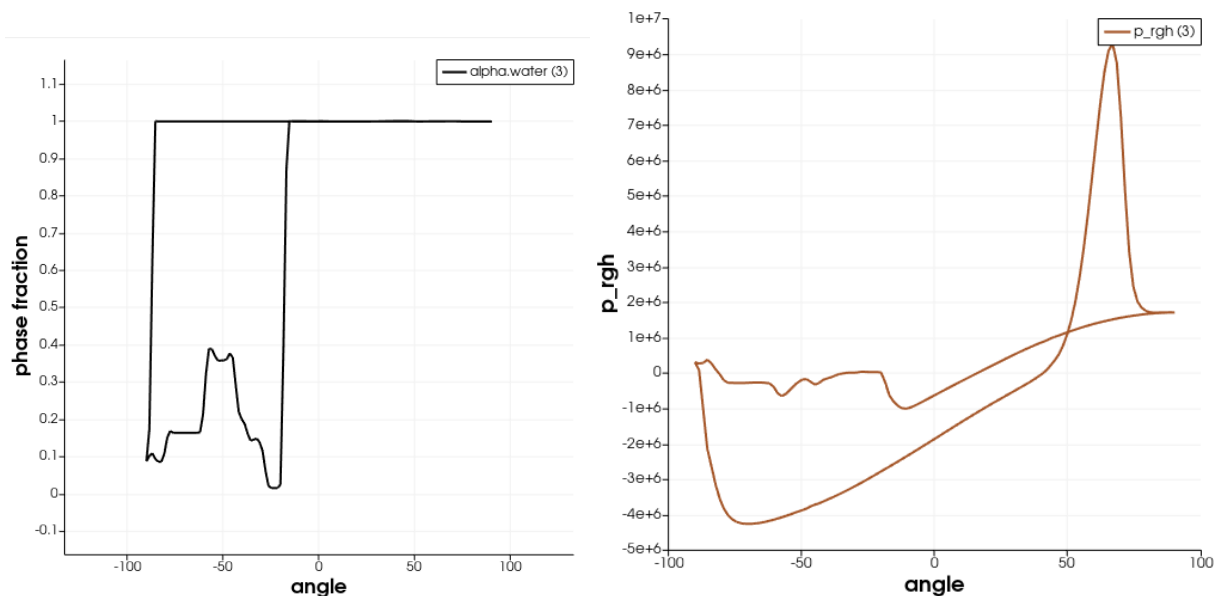


Figure 14: Plot of phase fraction(α) and hydrostatic pressure vs angle (θ)

Hydrostatic pressure and phase fraction is plotted against angle of cylinder as shown in Figure. 5 in order to study the angle of separation of fluid from the curved surface of the cylinder. Adverse pressure gradient and low value of phase fraction may be the indicator to know the angle of separation. Hence, from the plot it can be observed that at $\theta_1 = -12^\circ$ (or equivalently 192°) and $\theta_2 = -76^\circ$ (or equivalently 284°), i.e. at 192° and 284° fluid is separated at this point at 30 second.

Conclusions

The complete attachment of different viscous fluids at the curved cylinder surface took place at different interval of time. The fluids having more viscosity is observed to attain this nature faster however, the fluids having viscous range of more than 10^{-5} is observed to deviate from the regular pattern slightly and complete entrainment of cooking oil with the surface is achieved faster than SAE-30 and SAE-50 fluids despite their viscosity.

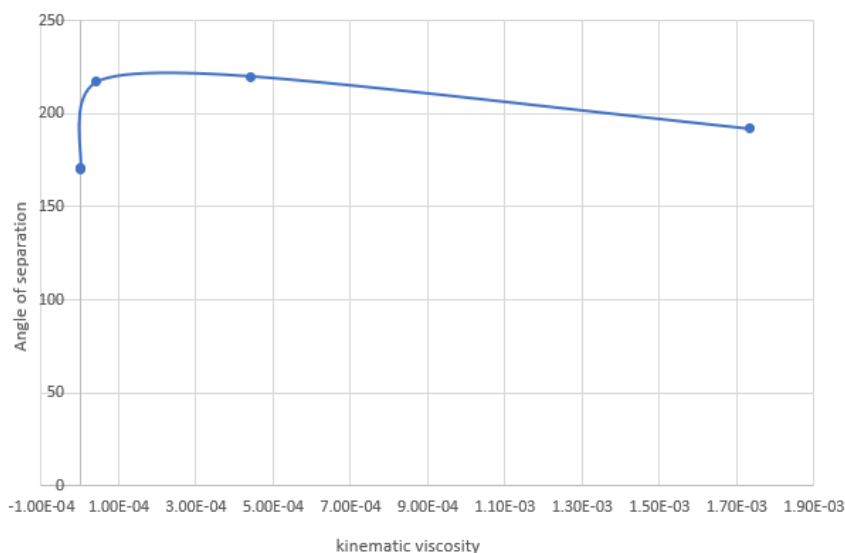


Figure 15: Plot of Angle of separation (in degrees) vs kinematic viscosity

The angle (θ) of the curved surface at which the fluid deviates has been observed at $t=30s$ for different viscous fluids. Higher viscosity of the fluid, more the jet sticks along the curved surface. This nature can be observed for the fluid with viscosity in the order of less than 10^{-5} , however, unusual trend is seen for the fluid having the viscosity in the range greater than 10^{-5} .

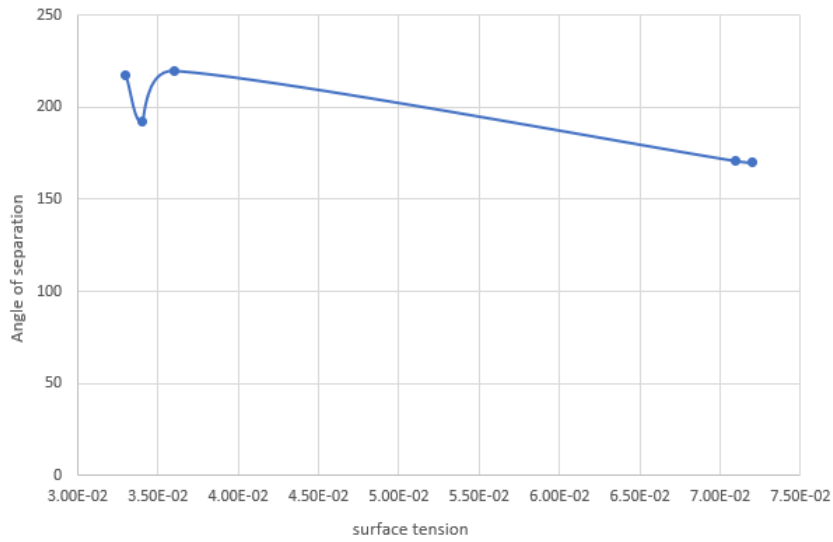


Figure 16: Plot of Angle of separation (in degrees) vs surface tension

The reason behind the deviation may be due to presence of surface tension between working fluid and ambient fluid since, surface tension also may play role in the Coanda effect.

References

- [1] *Mathematical Modelling and Numerical Investigations on the Coanda Effect* by A.Dumitrache, F. Frunzulica and T.C. Ionescu (<http://dx.doi.org/10.5772/50403>)
- [2] S. M. Damian. Description and utilization of interfoam multiphase solver. *International Center for Computational Methods in Engineering*, 2012.
- [3] D. J. Tritton. *Physical fluid dynamics*. Springer Science & Business Media, 2012.
- [4] R. Wille and H. Fernholz. Report on the first european mechanics colloquium, on the coanda effect. *Journal of Fluid Mechanics*, 23(4):801–819, 1965.
- [5] Sawyer RA. Two dimensional reattaching jet flow including the effect of curvature on entrainment. *Journal of Fluid Mechanics* 1963; 17 481-498.
- [6] Williams JC., Cheng EH., Kim KH. Curvature effects in a laminar and turbulent free jet boundary. *AIAA Journal* 1971; 4 733-736.